SYMCOMP 2017
Guimarães, 6-7 April 2017

MUSCL VS MOOD TECHNIQUES TO SOLVE THE SWE IN THE FRAMEWORK OF TSUNAMI EVENTS

Cláudia Reis[1]*, Jorge Figueiredo[1], Stéphane Clain[1], Rachid Omira[2], Maria Ana Baptista[3], Jorge Miranda[2]

1: Centre of Mathematics
School of Sciences
University of Minho
Campus de Gualtar, 4710 - 057 Braga
e-mail: claudiavdreis@sapo.pt, jmfiguei@math.uminho.pt, clain@math.uminho.pt
web: http://www.cmat.uminho.pt

2: Portuguese Institute for Sea and Atmosphere
Rua C do Aeroporto, 1749-077 Lisboa
e-mail: omirarachid10@yahoo.fr, miguel.miranda@ipma.pt

3: High Institute of Engineering of Lisbon
Lisbon Polytechnic Institute
R. Conselheiro Emídio Navarro 1, 1959-007 Lisboa
e-mail: mavbaptista@gmail.com

Keywords: Finite volume, MUSCL, MOOD, Japan 2011.

Abstract *The risk mitigation associated with tsunami events needs robust and accurate numerical tools to provide realistic solutions. We propose a comparative study between the efficiency of a finite volume numerical code, with second-order discretization in space and time, equipped with two different techniques to solve the non-conservative shallow-water equations: 1) the MUSCL (Monotonic Upstream-Centered Scheme for Conservation Laws) and, 2) the MOOD (Multi-dimensional Optimal Order Detection). A benchmarking process is carried out to validate the code. A one-dimensional simulation is performed to compare the MUSCL method equipped with the van Leer limiter, and the MOOD technique. We show that: 1) the quality of the solution may genuinely interfere with the scenario one wants to assess and, 2) the numerical tool equipped with the MOOD technique provides better solutions in comparison with the MUSCL results. At last, we apply and compare the two techniques to the real-case scenario Tohoku-Oki (Japan), 2011 tsunami.*

1. INTRODUCTION

Numerical tools, using non-linear hydrostatic shallow-water (NLHSW) models, are widely used to perform earthquake generated tsunami simulations in order to predict the tsunami behavior and build hazardous tsunami scenarios.
In this study, we present a finite volume numerical code, solving the NLHSW equations with second-order discretization in time and space and compare its performance considering two different techniques: Monotonic Upstream-Centered Scheme for Conservation Laws (MUSCL) [1] and Multi-dimensional Optimal Order Detection (MOOD) [2].
The MUSCL technique is based on *a priori* evaluation. The local linear reconstruction of the state variables is corrected using limiters to ensure that the Total Variation Diminishing (TVD) properties hold. The MOOD technique is based on *a posteriori* evaluation. A candidate solution is computed without any limitation using local polynomial reconstruction. If the solution fails to meet some stability criteria, the polynomial degree is decremented before recomputing the solution.
The performance of the numerical code was validated using the recommendations from the National Oceanic and Atmosphere Administration [3] and the studies of Synolakis et al. [4] and Tinti et al. [5]. The benchmarking process is fully described in Clain et al. [6]. In this paper, we show the code performance against a mathematical and a geophysical benchmark.
The mathematical benchmark consists of a one-dimensional dam-break involving an irregular bathymetry with no dry zones, to test and validate the code capacities to deal with complex topographies. Numerical simulations are carried out with MUSCL and MOOD techniques, using different mesh sizes (*i.e.* the number of cells), to test the convergence of the solution.
The geophysical benchmark involves the comparison between the one-dimensional analytical formula proposed by Carrier and Greenspan [7] with the results (amplitude and velocity) obtained for the numerical simulation of a wave propagating on a uniformly sloping beach, the corresponding L^1- and L^∞-errors being evaluated for both techniques.
The satisfactory results on the benchmarking process encourage us to move towards a real-case, the Tohoku-Oki tsunami that struck the coast of Japan in 2011. We performed a one-dimensional simulation, along two different profiles extending from the source area to the target coast, aiming at reproducing the tsunami behavior, using the different second-order methods (MUSCL and MOOD). The quality of the numerical solutions along the two profiles is analyzed and compared.
We show: 1) the advantage of the MOOD technique with respect to MUSCL technique; and 2) that the quality of the numerical solution may genuinely interfere with the scenario one wants to assess.

2. MODELING AND NUMERICAL SCHEMES

The two-dimensional shallow-water system with varying bathymetry is given in Cartesian coordinates by equations (1.1) - (1.3):

$$\partial_t h + \partial_x(hu) + \partial_y(hv) = 0, \tag{1.1}$$

$$\partial_t(hu) + \partial_x\left(hu^2 + \frac{g}{2}h^2\right) + \partial_y(huv) = -gh\partial_x b, \tag{1.2}$$

$$\partial_t(hv) + \partial_x(huv) + \partial_y\left(hv^2 + \frac{g}{2}h^2\right) = -gh\partial_y b, \tag{1.3}$$

where h, u, v, b represent the water height, the velocity components following respectively the x and y axis, and the bathymetry, while $g = 9.81ms^{-2}$ is the gravitational acceleration constant. In the following, $\eta = b + h$ will stand for the total water height (or free surface). A one-dimensional version consists in considering just equations (1.1) and (1.2) with $v = 0$. Numerical schemes for solving the non-conservative shallow-water system have to respect some fundamental principles: mass conservation and preservation of some critical steady-states, such as the lake at rest, at the discrete level (well-balanced scheme). The finite volume method turns out to be a very efficient technique to numerically compute an approximation and we refer to Clain et al. [6] for a detailed description. Here, we just outline the method for the sake of consistency.

2.1. Numerical method

Since the one- or two-dimensional problem involves uniform grids, we only give a description of the method for axis x and denote by C_i a cell with center x_i and length Δx, while $x_{i-\frac{1}{2}} = x_i - \Delta x/2$, $x_{i+\frac{1}{2}} = x_i + \Delta x/2$ are the cell interfaces. For a generic function φ, we denote by $\varphi_i \approx \varphi(x_i)$ the numerical approximation of φ at x_i, while $\varphi_{i+\frac{1}{2},L}$ and $\varphi_{i+\frac{1}{2},R}$ stand for approximations on the left and right side of interface $x_{i+\frac{1}{2}}$, respectively. When the two values are equal, we use the notation $\varphi_{i+\frac{1}{2}}$ since no distinction between the left and right side of the interface is needed.

Assuming that all the state variables are known at time t^n, we compute their new values at x_i and time t^{n+1} using the following finite volume scheme:

$$U_i^{n+1} = U_i^n - \frac{\Delta t}{\Delta x}\left(F_{i+\frac{1}{2}}^n + \varepsilon_{i+\frac{1}{2},L}^n - F_{i-\frac{1}{2}}^n - \varepsilon_{i-\frac{1}{2},R}^n\right) + \Delta t S_i^n, \tag{2}$$

where $F_{i+\frac{1}{2}}^n$ is the conservative flux across the interface $x_{i+\frac{1}{2}}$ while $U_i^n = (h_i^n, h_i^n u_i^n)$ is the vector of conservative variables. The source term S_i^n represents the discretization of the regular variation of the bathymetry, whereas $\varepsilon_{i+\frac{1}{2},L}^n$ and $\varepsilon_{i-\frac{1}{2},R}^n$ are the non-conservative flux contributions associated to the bathymetry discontinuity across the interface. Expressions for the source term and flux evaluations are given in Clain et al. [6] depending on the states computed on the left and right of the interface. Namely, for give values $h_{i+\frac{1}{2},L}, h_{i+\frac{1}{2},R}, u_{i+\frac{1}{2},L}, u_{i+\frac{1}{2},R}, b_{i+\frac{1}{2},L}, b_{i+\frac{1}{2},R}$ at time t^n, we compute the reconstructed hydrostatic states for interface $x_{i+\frac{1}{2}}$ in the following way. We denote by $b_{i+\frac{1}{2}}^* = \max(b_{i+\frac{1}{2},L}, b_{i+\frac{1}{2},R})$ the hydrostatic reconstruction bathymetry and set $h_{i+\frac{1}{2},L}^* =$

$\max(0, h_{i+\frac{1}{2},L} + b_{i+\frac{1}{2},L} - b^*_{i+\frac{1}{2}})$. We do the same for $h^*_{i+\frac{1}{2},R}$ which represents the effective water height in contact at the interface. We deduce $\eta^*_{i+\frac{1}{2},L} = h^*_{i+\frac{1}{2},L} + b^*_{i+\frac{1}{2}}$ (similarly for $\eta^*_{i+\frac{1}{2},R}$) the hydrostatic reconstruction free surface, while we denote $u^*_{i+\frac{1}{2},L} = u_{i+\frac{1}{2},L}$, $u^*_{i+\frac{1}{2},R} = u_{i+\frac{1}{2},R}$ for the sake of simplicity. We proceed in the same way for interface $x_{i-\frac{1}{2}}$. We then compute the fluxes $F^n_{i+\frac{1}{2}}$ and $F^n_{i-\frac{1}{2}}$ as well as the source term S^n_i with the reconstructed variables, while the non-conservative fluxes $\varepsilon^n_{i+\frac{1}{2},L}$ and $\varepsilon^n_{i-\frac{1}{2},R}$ use the differences between the original variables and the hydrostatic reconstructed ones.

2.2. MUSCL vs MOOD

At this stage, we have to define the state of the left and right side of the interface, $\varphi_{i+\frac{1}{2},L}$ and $\varphi_{i-\frac{1}{2},R}$, from the states φ_i in the cells (we skip the time index for the sake of simplicity). The first-order scheme simply consists of setting $\varphi_{i-\frac{1}{2},R} = \varphi_{i+\frac{1}{2},L} = \varphi_i$ but the numerical method would suffer of a high amount of numerical diffusion. To improve the accuracy, the MUSCL method is usually employed due to its simplicity. Unfortunately, the resulting scheme may still suffer of numerical diffusion and instabilities may appear since the original method has been designed for conservative problems and not for the non-conservative equations. We propose an alternative based on the MOOD technique [8][9] which is more stable and accurate. We give hereafter a short overview of the two methods.

The MUSCL technique consists in a piecewise linear reconstruction controlled by a limiting procedure to ensure some stability properties such as positivity preserving and TVD [1]. To this end, we set:

$$\varphi_{i-\frac{1}{2},R} = \varphi_i - \frac{\Delta x}{2}\varphi'_i, \qquad \varphi_{i+\frac{1}{2},L} = \varphi_i + \frac{\Delta x}{2}\varphi'_i, \tag{3}$$

with φ'_i an approximation of the derivative of the function corrected by a limiting procedure to avoid the creation of spurious oscillations leading to non-physical approximations. Limiters such as minmod [10], van Albada [11] and van Leer [12] are often used. In the present work we use the van Leer limiter.

The MOOD technique is based on a complete different paradigm [8][9]. The principle is to compute a candidate solution for time t^{n+1} using the linear reconstruction without any limitation. Then, we check if the solution is admissible, in a sense we shall detail further on, and if there are problematic cells they are "cured" to provide an admissible approximation. Thus, the MUSCL technique is an *a priori* method since we perform the reconstruction limitation with the value at time t^n whereas the MOOD technique is an *a posteriori* method since the correction is carried out in function of the candidate solution at time t^{n+1}. The main advantage is that the MOOD method is less restrictive since we only perform the limitation for the cells which present some oscillations leading to a more accurate approximation. We now introduce the basic concepts to define the MOOD method.

Cell Polynomial Degree (CPD). For each cell, we associate a value, named the CPD, setting: 1 for linear reconstruction (the default) and 0 for constant value. We then determine the values on the left and right sides of the interfaces with:

- If CPD[i]=0, we set $\varphi_{i-\frac{1}{2},R} = \varphi_{i+\frac{1}{2},L} = \varphi_i$. (4.1)

- If CPD[i]=1, we set $\varphi_{i-\frac{1}{2},R} = \varphi_i - \frac{\Delta x}{2}\varphi_i'$, $\varphi_{i+\frac{1}{2},L} = \varphi_i + \frac{\Delta x}{2}\varphi_i'$, (4.2)

  where we take: $\varphi_i' = \frac{\varphi_{i+1}-\varphi_{i-1}}{2\Delta x}$. (4.3)

The CPD map provides the information on the reconstructions we use to compute the candidate solution and we seek the best CPD map (higher degree) such that we have both accuracy and stability. To obtain a CPD map evaluation leading to an admissible solution at time t^{n+1} we proceed in the following way. For a given approximation (U_i^n) at time t^n and a prescribed CPD map, we compute a candidate solution $\left(U_i^{\#}\right)$ using the polynomial reconstruction given by the CPD map. Then, an iterative procedure involving a certain number of detectors (see below) is set to provide an admissible solution.

Detector. A detector is a small routine that checks a specific property of the candidate solution. We list hereafter three simple detectors we employ in the code:

Physical Admissible Detector (PAD). We say that approximation $U_i^{\#}$ on cell C_i is physically admissible if $h_i^{\#} \geq 0$. If the cell does not satisfy such a criterion, we set CPD[i] =0.

Extremum Detector (ED). We say that approximation $U_i^{\#}$ on cell C_i presents a local extremum if $h_i^{\#} > max(h_{i-1}^{\#}, h_{i+1}^{\#})$ or $h_i^{\#} < min(h_{i-1}^{\#}, h_{i+1}^{\#})$. If that is the case, we label cell C_i as problematic.

Smoothness detector (u2). When the candidate solution is considered problematic (*i.e.* presents an extremum on cell C_i), the local curvature χ_i is evaluated numerically as well as on the neighbor cells C_j.

- If the curvatures have opposite signs then the cell is not eligible and we set CPD[i]=0.
- If the absolute value of ratio $\frac{\min(|\chi_{i-1}|,|\chi_i|,|\chi_{i+1}|)}{\max(|\chi_{i-1}|,|\chi_i|,|\chi_{i+1}|)}$

  is too small with respect to a given threshold, the cell is not eligible and we set CPD[i]=0.
- Otherwise, we say that the candidate solution satisfies the u2 criterion and the solution for that cell is considered admissible (CPD[i]=1).

If the CPD map has been altered, we compute again the candidate solution for the cells that have been corrected and for their neighbor cells only. Otherwise, the candidate solution turns out to be the solution at time t^{n+1}. It has been shown that this procedure always provides an admissible solution [13] free from non-physical oscillations.

3. TEST CASES

In our code validation process, mass conservation, convergence, stability and the well-balanced property (or C-property) were considered and positively assessed [6]. Several benchmarks were carried out to perform the verification and validation of the numerical scheme, through comparisons of the code predictions with analytical solutions, laboratory experiments and field measurements [6].
This section is devoted to the synthetic benchmarks in order to assess the advantages of the MOOD technique with respect to the MUSCL one. The first test corresponds to a classical dam-break involving shocks and rarefactions (see [14] and references therein) to draw comparisons when discontinuities are involved. The second test case corresponds to an analytical benchmark [3][4] based on a one-dimensional smooth solution of an initial value problem for a single wave nonlinear propagation over a constant slope beach [7]. It belongs to the set of test cases proposed in the technical memorandum from the National Oceanic and Atmosphere Administration [3], based on the Long Wave Run-Up Models Workshops [15][16][17].

3.1. Dam-break

The first benchmark consists of a one-dimensional dam-break involving an irregular bathymetry with no dry zones. The simulation domain is $[0\text{m}, 1\text{m}]$ and the initial configuration is such that the water level is 1m for $x \in [0m, 0.5\text{m}]$ and 0.05m otherwise. The discontinuous bathymetry corresponds to a ramp located at $x \in [0.65m, 0.75\text{m}]$ with a slope coefficient of 0.4 as presented in Figure 1.

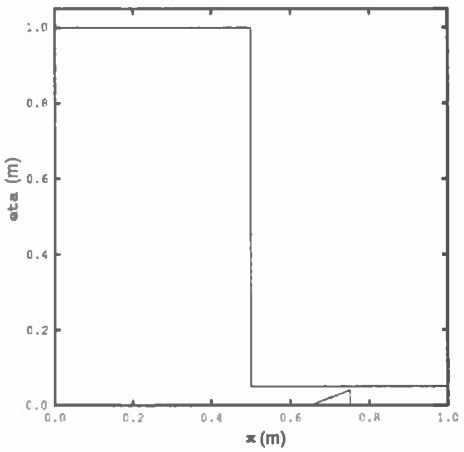

Figure 1. Dam-break: representation of bathymetry and initial configuration for the water free surface.

The system is initially at rest and the simulation is carried until a final simulation time $t_f = 0.125\text{s}$ is reached. Reflection boundary conditions are prescribed for both domain sides. Since no analytical solution is available for comparison, we consider a reference

solution obtained with the first-order scheme and a uniform mesh of 100 000 cells. The numerical simulations are carried out with the MUSCL and the MOOD methods for two uniform meshes of 100 and 200 cells. The conservative numerical flux is computed with the HLL law while the non-conservative flux derives from the hydrostatic reconstruction formalism presented in the previous section.
The water free surface and the velocity field obtained using the MUSCL and the MOOD techniques at the final time $t = t_f$ are plotted in Figure 2 for the 100 and the 200 cells case together with the corresponding reference numerical solution.

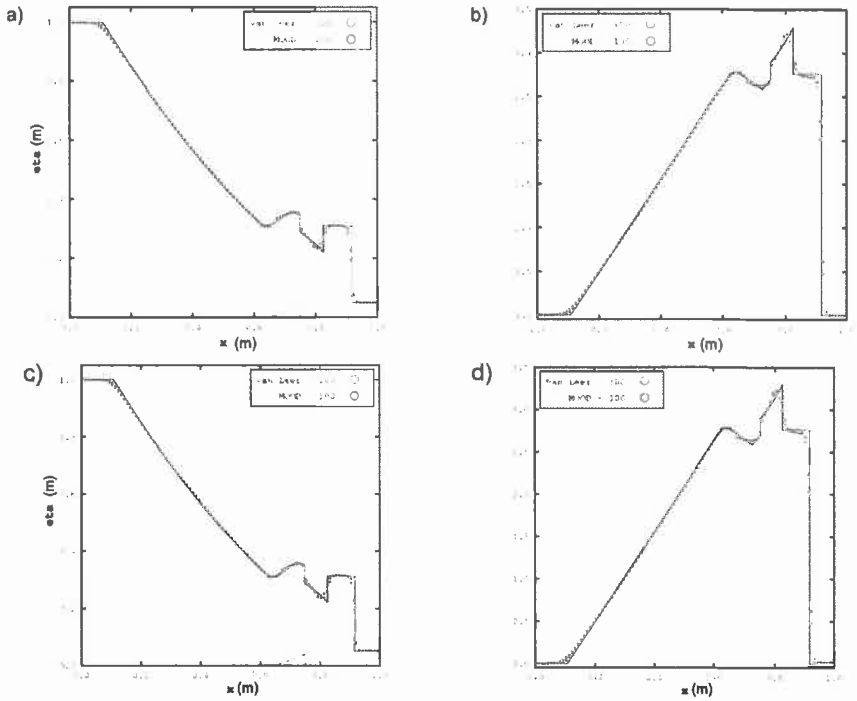

Figure 2. Dam-break: comparison between the reference numerical solution (solid line) and the numerical solutions obtained with the MUSCL method (red circles) and the MOOD method (blue circles). a) Water free surface at $t = t_f$ for the 100 mesh. b) Water velocity at $t = t_f$ for the 100 mesh. c) Water free surface at $t = t_f$ for the 200 mesh. d) Water velocity at $t = t_f$ for the 200 mesh.

We report that the MOOD method provides the best approximation since it better fits the reference curve. The two rarefactions feet situated at $x = 0.15m$ and $x = 0.65m$, corresponding to the beginning and the end of the rarefaction, are very sensitive to the numerical diffusion since they correspond to singular points involving a discontinuity of the derivative. The MUSCL curve presents a rather smeared shape whereas the MOOD curve really catches well the singular points. Such a good behavior of the MOOD technique is noticeable since the evaluation of the solution at these specific points represents a real

difficulty from the numerical point of view. On the other hand, an important challenge is to capture the shocks with very few points. The genuinely nonlinear shocks right after $x = 0.8m$ and $x = 0.9m$ are very well recovered by the two techniques but MOOD turns out to be better since the curve manages to reach the peak of the reference solution. At last, convergence in mesh has been checked and the 200 cells mesh provides a satisfactory improvement with respect to the 100 cells one, particularly for the rarefaction. Additionally, numerical experiences with finer grids (not presented here) have been carried out allowing to validate the convergence in mesh property.

3.2. Single wave on a sloping beach

We perform a one-dimensional analytical benchmark where dry and wet zones are involved. A wave of given initial profile and initial null velocity propagates over a constant-slope beach. The leading-depression N wave travels across a 1/10 slope and we compare the numerical solution with the one obtained by the analytical integral formula given by Carrier and Greenspan [7] and Carrier et al. [18]. We consider the domain$[-570\text{m}, 30\text{m}]$, where the subdomain $[0\text{m}, 30\text{m}]$ corresponds to the region that is initially dry (i.e. $x = 0\text{m}$ corresponds to the shoreline position at $t = 0\text{s}$). The domain is discretized using a uniform mesh having 600 cells.

Figure 3 depicts, for $t = 13\text{s}$, the free surface using MUSCL and MOOD methods (global view and a zoom close to the dry/wet interface to assess the accuracy of the two second-order simulations).

We report that the solution obtained with the MOOD technique is more accurate in comparison with the solution obtained with the MUSCL technique.

a)

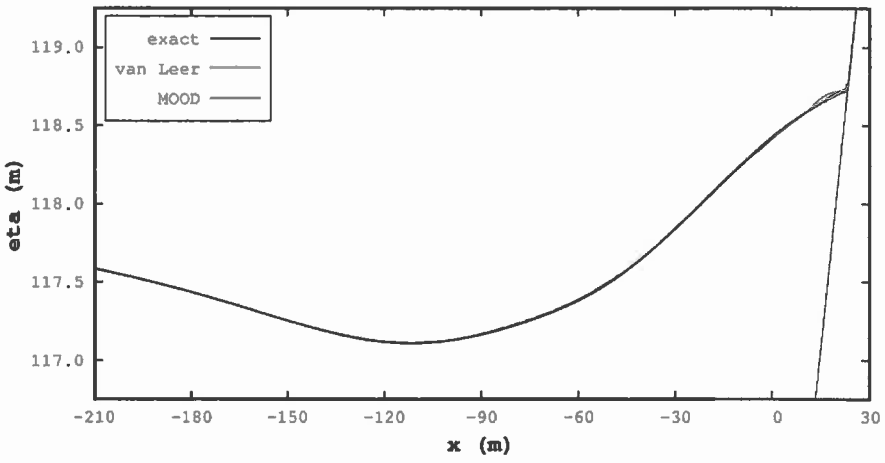

b)

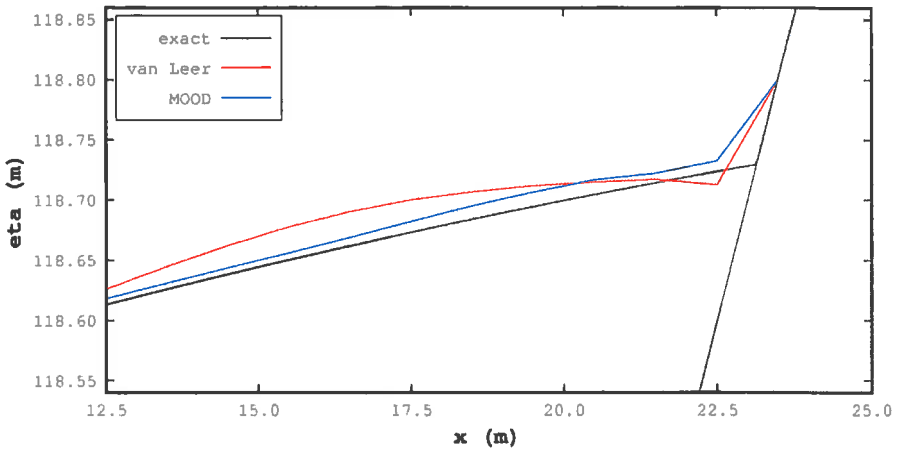

Figure 3. Sloping beach: comparison between the exact solution and the numerical simulations for the water free surface η at t = 13s. The exact solution is presented together with the numerical ones: a) Global view; b) Zoom close to the dry/wet interface.

Table 1 quantifies the accuracy by evaluating the maximum error ε_η^∞ and the L^1-error ε_η^1 on the free surface elevation (see [6], for the definition of the metrics). Evaluation of the free surface obtained with the MOOD technique provides a clear improvement over the MUSCL solution.

Scheme	Free surface		Velocity	
	ε_η^∞	ε_η^1	ε_u^∞	ε_u^1
MUSCL	2.82×10^{-2}	1.62×10^{-3}	3.04	7.62×10^{-3}
MOOD	1.27×10^{-2}	1.05×10^{-3}	1.96×10^{-1}	1.73×10^{-3}

Table 1. Sloping beach: Errors for the free surface and velocity for t = 13s using two metrics.

Figure 4 depicts the exact analytical solution for the velocity and the simulated approximations at t = 13s.
The MOOD technique results are more accurate than the results obtained with the MUSCL technique. Table 1 provides a numerical quantification of the errors on the velocity for the two schemes. Notice that the approximation obtained with the van Leer scheme is particularly problematic. The reason is that we are dealing with a non-conservative problem and the computation of the velocity is very sensitive.
Evaluation of the velocity is one of the most difficult parts of the numerical scheme in presence of small water height. The L^1 metric shows that the MOOD method is better, whereas the MUSCL technique suffers of a large deviation.

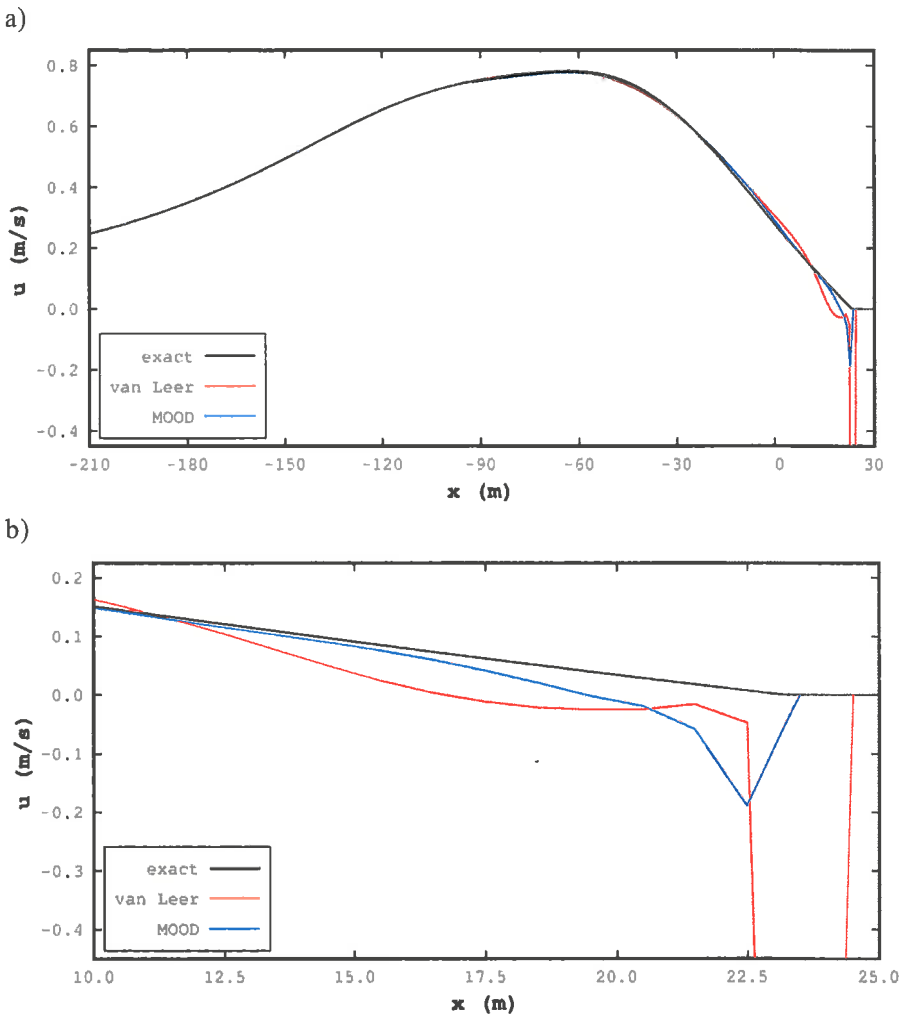

Figure 4. Sloping beach: comparison between the exact solution and the numerical approximations for the velocity u at t = 13s. The exact solution is presented together with the numerical ones: a) Global view; b) Zoom close to the dry/wet interface.

Both test cases (3.1 and 3.2) show that the MOOD technique provides a better approximation to the solution than the MUSCL approach, with sharper shock capture and less numerical diffusion.

4. REAL-CASE STUDY

At 14:46:18.1 local time (5:46:18.1 UTC), on March 11, 2011, a magnitude Mw9.0 tsunamigenic earthquake occurred in Japan: The earthquake epicenter (38.1035°N,

142.861°E) and depth (24 km) were estimated by the Japan Meteorological Agency (JMA) (see Figure 5). Multiple sea-level sensors recorded the event, namely the Deep-ocean Assessment and Reporting of Tsunamis (DART) and the Global Positioning (GPS) systems (Figure 5).

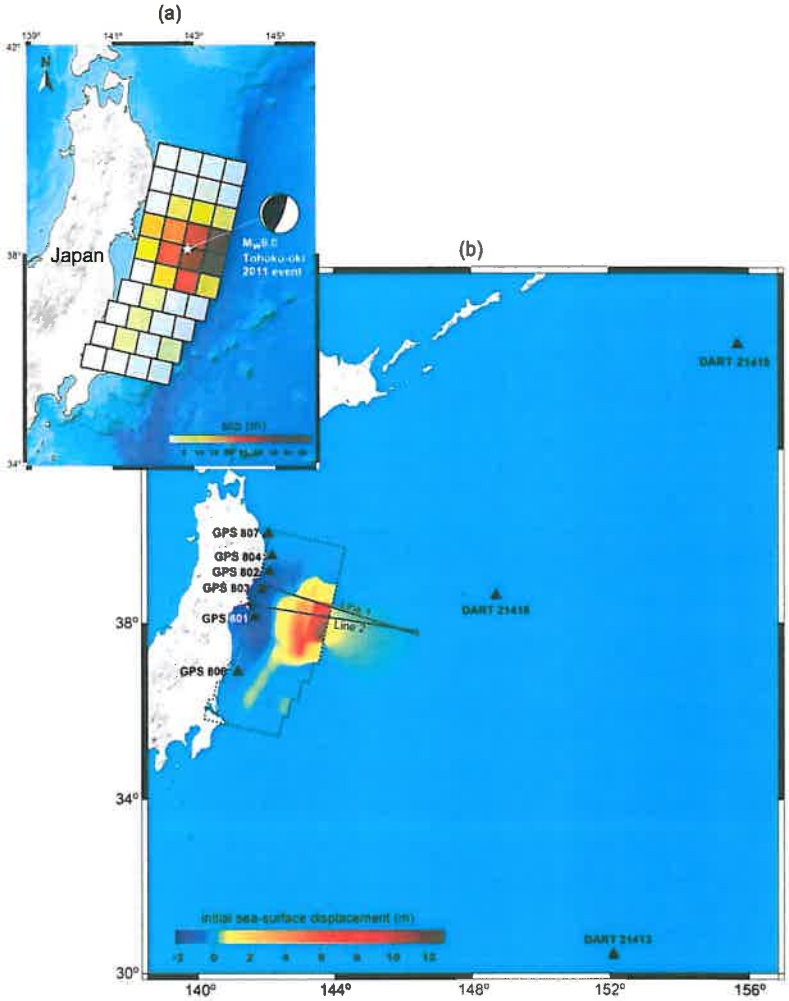

Figure 5. Tohoku-Oki, 2011, earthquake and tsunami model: a) Co-seismic slip distribution proposed by Fujii et al. [19], location of the epicenter (white star) and focal mechanism (beach ball) determined by JMA; b) The modeled sea-surface displacement caused by the Tohoku-Oki, 2011 earthquake. Black triangles represent the locations of the sea-level sensors. Lines 1 and 2 represent the profiles location used in the 1D simulation.

4.1. Tsunami generation

To simulate the tsunami wave creation caused by the 2011 Tohoku-Oki earthquake, we use

the source model proposed by Fujii et al. [19]. This finite-fault model considers heterogeneous slip distribution and constitute the base to define the tsunami initial conditions. Figure 5a depicts the heterogeneous slip distribution along the rupture area of the 2011 Tohoku-Oki earthquake fault as determined by Fujii et al. We calculate the co-seismic vertical displacements through the half space elastic theory [20] and transfer the vertical deformations corresponding to the sea-floor to the free ocean surface with the assumption that both deformations of sea bottom and ocean surface are equal [21]. The bathymetry model used for the tsunami simulation is from the General Bathymetric Chart of the Oceans (GEBCO) 30-arc sec gridded data (available at: http://www.gebco.net/). Figure 5b depicts the initial sea-surface displacement caused by the 2011 Tohoku-Oki earthquake.

4.2. One-dimensional simulation for code techniques comparison

The goal of this section is twofold: 1) show that a one-dimensional numerical model is appropriate to describe the wave propagation is some situations; and 2) show that the MOOD method is more efficient than the MUSCL method to provide a stable and accurate numerical approximation of the wave propagation.

4.2.1. Model reduction to one-dimensional problem

We extract two profile lines (labelled 1 and 2) from the two-dimensional map (see Figure 5b) joining the tsunami origin with the coastline such that the lines are essentially orthogonal to the direction of the waves' propagation. Such a model reduction is effective assuming that the waves preserve their unidimensional shape. Therefore, to ensure physical coherence between the two- and the one-dimensional models, the available potential energy of the one-dimensional initial water at rest configuration is changed by reducing the water height so that both two-dimensional and one-dimensional numerical models lead to the same maximum water elevation at approximately 10km from the initial configuration of the shoreline ($x = 0$m). The one-dimensional mesh of each line is uniform and inherited from the two-dimensional mesh, the cell length being approximately 364m for line 1 and 353m for line 2. Numerical simulations are carried out up to a simulation final time $t_f = 50$min.
To assess the quality of the correspondence between the two- and the one-dimensional numerical models when the MUSCL scheme is used we consider 10 reference points along each line, spanning approximately from $x = 90$km to $x = 3$km. For each reference point, we look at the absolute difference between the results given by the two- and the one-dimensional simulations for the maximum free surface level and the corresponding time. The results obtained for line 1 (line 2 resp.) lead to deviations for the maximum free surface level with average 7.5% (2.5% resp.) and maximum 12.7% (3.4% resp.), while for the corresponding time we obtain differences with average 0.8% (4.7% resp.) and maximum 1.6% (11.4% resp.), being all deviations smaller close to the shoreline.
The one- and the two-dimensional models fit very well and confirm that the unidirectional model is relevant to analyze the run-up.

4.2.2. Comparison between the two high-order strategies

We have carried out several benchmarks to assess the quality of the numerical solutions considering two types of conditions for the wave-coast interaction (see Table 2):

- The run-up assumption, where the wave meets a sloping beach and spreads until it reaches a zero velocity;
- The cliff condition, where the wave meets a high cliff preventing the tsunami from entering in the dry area.

For the run-up and cliff conditions, we consider, for different points along lines 1 and 2 near the shoreline, the maximum water elevation η_{max} and the associated time t_{max} when the MUSCL and the MOOD numerical schemes are used. The maximum shoreline water elevation and the corresponding time, as well as the maximum inshore distance reached by the wave were also considered for the run-up case.
The results obtained show that the time corresponding to the maximum water elevation does not change significantly when different numerical schemes are considered for both line 1 and line 2.
We report that the MOOD scheme systematically leads to greater values of the maximum water elevation both in the wet zone and on the shoreline. In the run-up simulation, this difference amounts up to almost 1 and 2 meters, respectively at the shoreline and at $x = 0$m. This difference can reach almost 3 meters in the cliff condition scenario. From a practical point of view, a difference of 3 meters may result in rather catastrophic consequences. Indeed, a protection infrastructure such as a seawall designed on the basis of the MUSCL simulations will be underestimated while the MOOD method predicts that the water may overtop the infrastructure. For long-time simulation like the tsunami propagation, MUSCL technique is much diffusive and provides an underestimation of the wave height when reaching the coast. The MOOD method is less diffusive and gives more realistic estimates of the free-surface height.

5. CONCLUSIONS

We have developed a finite volume scheme and implemented the corresponding C++ code, with resolution up to second-order, hydrostatic reconstruction, well-balanced property and two high-order techniques: MUSCL and MOOD.
The solution quality achieved with the numerical tool is of utmost importance for the tsunami risk mitigation. In this study, the quality solutions were evaluated and compared in a benchmarking process and a real-case scenario, the Tohoku-Oki, 2011 event.
The analytical benchmarks used to validate the code show a better performance of the MOOD technique with respect to the MUSCL one.
The two-dimensional bathymetric and tsunami initial deformation models were used to calibrate the one-dimensional model for two profiles coinciding with two tide gauges. The unidimensional simulation was performed using the MUSCL and MOOD techniques to assess the accuracy. It brought out that the MUSCL method is too much diffusive for long-time simulation, providing underestimation of the water height whereas the MOOD method

manages to give a more realistic evaluation.
The results of the benchmarking process show that: 1) the first-order simulation presents the less accurate numerical solution, mostly due to diffusion; 2) the MUSCL limiters have influence on the numerical solution; and 3) MOOD provides the best numerical solution.

Run up condition									
Line 1					Line 2				
Point	MUSCL		MOOD		Point	MUSCL		MOOD	
x	η_{max}	t_{max}	η_{max}	t_{max}	x	η_{max}	t_{max}	η_{max}	t_{max}
-9.83	5.8	29.9	6.9	29.8	-10.66	9.8	33.9	10.9	33.8
-7.65	6.1	30.9	7.2	30.8	-7.42	10.7	35.2	11.8	35.2
-5.10	6.9	32.1	8.0	31.9	-4.95	12.1	36.9	13.2	36.7
-2.55	7.8	33.4	8.8	33.1	-2.47	13.5	37.7	14.5	37.9
0.0	11.1	35.4	12.9	35.0	0.0	19.0	38.4	20.8	39.5
shoreline	17.6	35.6	14.1	35.5	shoreline	18.4	40.8	19.2	40.4
x_{max}	728m		364m		x_{max}	353m		353m	
Cliff condition									
Line 1					Line 2				
Point	MUSCL		MOOD		Point	MUSCL		MOOD	
x	η_{max}	t_{max}	η_{max}	t_{max}	x	η_{max}	t_{max}	η_{max}	t_{max}
-9.83	5.8	29.9	6.9	29.8	-10.66	9.8	33.9	10.9	33.8
-7.65	6.1	30.9	7.2	30.8	-7.42	10.7	35.2	11.8	35.3
-5.10	7.2	32.1	8.2	31.9	-4.95	12.1	36.9	13.2	36.7
-2.55	7.7	33.3	8.9	33.1	-2.47	13.5	37.7	14.5	37.9
0.0	12.5	34.8	14.5	35.0	0.0	18.8	39.7	21.4	39.7

Table 2. 1D tsunami simulation: Maximum water elevation η_{max} (in meters) and corresponding time t_{max} (in minutes) for MUSCL and MOOD numerical schemes for lines 1 and 2. The different points are identified by the corresponding x-coordinate (in kilometers). For the run-up condition, the results for the shoreline are also presented.

REFERENCES

[1] LeVeque, R.J. "Finite volume methods for hyperbolic problems". *Cambridge university press*, vol. 31, 2002.

[2] Clain, S., Figueiredo, J. "The MOOD method for the non conservative shallow-water system". *Computers & Fluids,* 145, 99-128, 2017.

[3] Synolakis, C.E., Bernard, E.N., Titov, V.V., Kanoglu, U., Gonzalez, F.I. "Standards, criteria and procedures for NOAA evaluation of tsunami numerical models". *NOAA Technical Memorandum OAR PMEL-135*, 2007.

[4] Synolakis, C.E., Bernard, E.N., Titov, V.V., Kânoğlu, U., González, F.I. "Validation and verification of tsunami numerical models". *Pure and Applied Geophysics*, 165(11-12), 2197-2228, 2008.

[5] Tinti, S., Tonini, R. "The UBO-TSUFD tsunami inundation model: validation and application to a tsunami case study focused on the city of Catania, Italy". *Nat. Hazards Earth Syst. Sci.*, 13, 1795-1816, 2013.

[6] Clain, S., Reis, C., Costa, R., Figueiredo, J., Baptista, M. A., Miranda, J. M. "Second-order finite volume with hydrostatic reconstruction for tsunami simulation". *Journal of Advances in Modeling Earth Systems*, 8(4), 1691-1713, 2016.

[7] Carrier, G.F., Greenspan, H.P. "Water waves of finite amplitude on a sloping beach". *Journal of Fluid Mechanics*, 4(01), 97-109, 1958.

[8] Diot, S., Clain, S., Loubère, R. "Improved detection criteria for the Multi-dimensional Optimal Order Detection (MOOD) on unstructured meshes with very high-order polynomials". *Computers & Fluids,* 64, 43-63, 2012.

[9] Diot, S., Loubère, R., Clain, S. "The MOOD method in the three-dimensional case: Very-High-Order Finite Volume Method for Hyperbolic Systems". *International Journal for Numerical Methods in Fluids*, 73(4), 362-392, 2013.

[10] Roe, P.L. "Characteristic-based schemes for the Euler equations". *Ann. Rev. Fluid Mech.*, 18, p337, 1986.

[11] Van Albada, G.D., Van Leer, B., Roberts, W.W. "A comparative study of computational methods in cosmic gas dynamics". *Astron. Astrophysics,* 108, p76, 1982.

[12] Van Leer, B. "Towards the ultimate conservative difference scheme. IV. A new approach to numerical convection". *Journal of computational physics*, 23(3), 276-299, 1977.

[13] Clain, S., Diot, S., Loubère, R. "A high-order polynomial finite volume method for hyperbolic system of conservation laws with Multi-dimensional Optimal Order Detection (MOOD)". *Journal of computational Physics*, 230, 4028-4050, 2011.

[14] Delestre, O., Lucas, C., Ksinant, P.A., Darboux, F., Laguerre, C., Vo, T.N.T., James, F., Cordier, S. "SWASHES: a compilation of shallow water analytic solutions for hydraulic and environmental studies". *Int. J. Numer. Meth. Fluids*, 74, 229-230, 2014.

[15] Liu, P.L.F., Synolakis, C.E., Yeh, H.H. "Report on the international workshop on long-wave run-up". *Journal of Fluid Mechanics*, 229, 675-688, 1991.

[16] Yeh, H., Liu, P., Synolakis, C.E. "Long-wave Runup Models: Friday Harbor, USA, 12-17 September 1995". *World Scientific*, 1996.

[17] Synolakis, C.E., Bernard, E.N. "Tsunami science before and beyond Boxing Day 2004". *Philosophical Transactions of the Royal Society of London A: Mathematical, Physical and Engineering Sciences*, 364(1845), 2231-2265, 2006.

[18] Carrier, G.F., Wu, T.T., Yeh, H. "Tsunami run-up and draw-down on a plane beach". *Journal of Fluid Mechanics*, 475, 79-99, 2003.

[19] Fujii, Y., Satake, K., Sakai, S.I., Shinohara, M., Kanazawa, T. "Tsunami source of the 2011 off the Pacific coast of Tohoku Earthquake". *Earth, planets and space*, 63(7), 815-820, 2011.

[20] Okada, Y. "Surface deformation due to shear and tensile faults in a half-space". *Bulletin of the seismological society of America*, 75(4), 1135-1154, 1985.

[21] Kajiura, K. "Tsunami source, energy and the directivity of wave radiation". *Bull. Earthq. Res. Inst.*, 48, 835–869, 1970.